Tracking the phase-transition energy in the disassembly of hot nuclei

C. B. Das,[1] S. Das Gupta,[1] L. Beaulieu,[2] T. Lefort,[3,*] K. Kwiatkowski,[3,†] V. E. Viola,[3] S. J. Yennello,[4] L. Pienkowski,[5] R. G. Korteling,[6] and H. Breuer[7]

[1]*Physics Department, McGill University, Montréal, Canada H3A 2T8*
[2]*Department de Physique, Université Laval, Quebec, Canada G1K 7P4*
[3]*Department of Chemistry and IUCF, Indiana University, Bloomington, Indiana 47405*
[4]*Department of Chemistry and Cyclotron Laboratory, Texas A&M University, College Station, Texas 77843*
[5]*Heavy Ion Laboratory, Warsaw University, 02-093 Warsaw, Poland*
[6]*Department of Chemistry, Simon Fraser University, Burnaby, British Columbia, Canada V5A 1S6*
[7]*Department of Physics, University of Maryland, College Park, Maryland 20742*

(Received 21 June 2002; published 7 October 2002)

In efforts to determine phase transitions in the disintegration of highly excited heavy nuclei, a popular practice is to parametrize the yields of isotopes as a function of temperature in the form $Y(z)=z^{-\tau}f(z^{\sigma}(T-T_0))$, where $Y(z)$'s are the measured yields and τ, σ, and T_0 are fitted to the yields. Here T_0 would be interpreted as the phase transition temperature. For finite systems such as those obtained in nuclear collisions, this parametrization is only approximate and hence allows for extraction of T_0 in more than one way. In this work we look in detail at how values of T_0 differ, depending on methods of extraction. It should be mentioned that for finite systems, this approximate parametrization works not only at the critical point, but also for first-order phase transitions (at least in some models). Thus the approximate fit is no guarantee that one is seeing a critical phenomenon. A different but more conventional search for the nuclear phase transition would look for a maximum in the specific heat as a function of temperature T_2. In this case T_2 is interpreted as the phase transition temperature. Ideally T_0 and T_2 would coincide. We invesigate this possibility, both in theory and from the ISiS data, performing both canonical (T) and microcanonical ($e=E^*/A$) calculations. Although more than one value of T_0 can be extracted from the approximate parametrization, the work here points to the best value from among the choices. Several interesting results, seen in theoretical calculations, are borne out in experiment.

DOI: 10.1103/PhysRevC.66.044602 PACS number(s): 25.70.−z, 25.75.Ld

I. INTRODUCTION

In studies of phase transitions in the disintegration of highly excited heavy nuclei, a popular path for deducing the occurrence of a phase transition is to examine the yields of composites. These are readily available from experimental data and hence have been the focus of many theoretical studies [1]. The usual practice is [2] to use a parametrization

$$Y(z)=z^{-\tau}f(z^{\sigma}(T-T_0)) \tag{1.1}$$

and extract values of τ, σ, and T_0, which occur in models of critical phenomena [2]. Here z is the charge of the composite, the parameters τ and σ are critical exponents, and T_0 is the critical temperature. Alternately, in a microcanonical formalism one would write

$$Y(z)=z^{-\tau}f(z^{\sigma}(e-e_0)). \tag{1.2}$$

Here $e=E^*/A$, the excitation energy per nucleon, and e_0 would be the phase transition energy. Formulas (1.1) and (1.2) assume that the thermodynamic limit is reached. In practice, in the nuclear case we have a finite system that disintegrates and thus the above parametrization is only approximate. Hence the values of the parameters can be extracted in more than one way and these values may not be the same. We point out that when the Coulomb force is considered different methods of extracting the phase transition energy yield dramatically different results.

Alternative but perhaps more common tools for studies of phase transition in other fields of physics are measurements of compressibility, specific heat, etc. Experimental data for specific heat were studied in the nuclear case and were indeed the cause of great excitement [3].

We have therefore two distinct ways of trying to deduce a phase transition energy: from the distribution of composites as the excitation energy is varied (as explained, even here there can be more than one value) or, what may be more difficult but achievable, to locate an extremum of the specific heat. We label the excitation energy at which the specific heat maximises as e_2. We will show that two ways of extracting e_0 from Eq. (1.1) or (1.2) lead to different values for this parameter. We will label them e_1 and e_1'. It is not obvious that the values of e_1, e_1', and e_2 are close, although from the seminal work of Coniglio and Klein [4] on cluster formation this result could be anticipated.

We have compared both approaches in the nuclear case in the framework of two models. Although the models are very different and each has its own strengths and weaknesses, both reveal the following interesting features. If we switch off the Coulomb interaction between protons, the deduced

*Present address: Laboratoire de Physique Corpusculaire de Caen, F-14050 Caen Cedex, France.
†Present address: Los Alamos National Laboratory, Los Alamos, NM 87545.

phase transition energies, e_1, e_1', and e_2, are close. With the inclusion of the Coulomb force, e_1 and e_1' begin to diverge. For a nucleus of the size of ^{197}Au, the case we study and for which fragmentation data exist, the difference in the values of e_1 and e_1' is significant. Furthermore, one of these values stays close to the value at which the specific heat maximizes and gives a good measure of the phase transition energy.

The two models we use are the lattice gas model (LGM) [1,5] and a thermodynamic model [6,7]. The second model is close in spirit to the statistical multifragmentation model of Copenhagen [8]. We choose to use a microcanonical simulation for LGM. So here the primary quantity is the excitation energy e per particle, and a temperature can be derived afterwards [9]. For the thermodynamic model, we do a canonical calculation so that the temperature is the primary parameter and an excitation energy e per particle can be derived afterwards.

In Sec. II we give details of the LGM calculations. Results of the thermodynamic model are presented in Sec. III. In Sec. IV we investigate the ISiS data within those formalisms. We present the summary and conclusion in Sec. V.

II. RESULTS FROM LGM

Numerical techniques for microcanonical simulations with LGM have been published [9]. Calculations are done for fixed $E=Ae$, where e is the excitation energy per nucleon. This is the primary quantity for simulations. The temperature for each simulation can be calculated from $T=\langle 2E_{\rm kin}\rangle/3$. This is discussed in detail in Ref. [9]. For more discussions about the LGM with Coulomb force we refer to Ref. [10], Sec. II. Bonds due to nuclear forces are taken to be -5.33 MeV between unlike particles and 0 between like particles. The LGM has several drawbacks, the most noticeable being the lack of quantum effects, which leads to an incorrect caloric curve near $T=0$. The LGM has the following advantages not shared by several other models. It includes interactions between composites. It incorporates the Coulomb interaction in a much more basic fashion (at the nucleonic level) than several other models. This is very important for us since this work points to a new effect brought about solely by the Coulomb interaction. Also the LGM produces particle-stable composites [10,11] so that the complicated problem of subsequent particle evaporation is circumvented.

All calculations reported here are for $Z=79$ and $N=118$ (^{197}Au). At each total energy we compute averages after 50 000 simulated events. We use 9^3 ($\rho/\rho_0=0.27$) lattice sites.

The extraction of parameters from yields [Eq. (1.2)] merits consideration. Discussions of this parametrization can be found in Ref. [2] where it is used to model a continuous phase transition in an infinite system. As already stated, one does not expect the above parametrization to be exact except in the thermodynamic limit. For very finite systems as is the case with disintegrating nuclei formed in very energetic nuclear collisions, the parametrization is only approximate and is by no means a signature of a critical phenomenon but rather that of a phase transition in a finite system, first order or otherwise [12]. The parametrization of Eq. (1.1) requires that the charge (z) not extend to extremely small values [2]. In the nuclear case it is also not too big since the disassembling system itself is quite small. We limit z between 3 and 17, which is similar to most published work on the subject. Since the fit is expected to be only approximate, there is more than one prescription for getting the ''best'' parameters. In the following five steps, we outline the procedure for extracting the values of e_1 and e_1' [13].

(1) If Eq. (1.2) were exact, then at $e=e_0$ we would have $\Sigma[\ln Y(z)-\ln C+\tau\ln z]^2=0$, as each individual term in the sum would be zero. Of course Eq. (1.2) is not exact and thus the sum above will not be zero at any value of e. However, the following are valid questions. At any given e how well does the distribution fit a power law and what is the value of τ that gives a best fit to a power law? At each e we get a ''best'' τ by a least-square fit, i.e., by minimizing $\Sigma[\ln Y(z)-\ln C+\tau\ln z]^2$ with respect to τ and C. The ''goodness'' of fit is given by the smallness of the sum, which we define to be χ^2 (there are other definitions of χ^2):

$$\chi^2\equiv\frac{1}{N}\sum\,[\ln Y(z)-\ln C+\ln z]^2. \tag{2.1}$$

Here N is the number of terms in the sum. From this step we have a ''best'' τ and a χ^2 vs e. One obvious choice of e_0 is that value of e where χ^2 is minimum (see Ref. [14]). The value of e_0 deduced using this criterion will be called e_1'. While this is quite reasonable, it does not make use of the scaling property $z^\sigma(e-e_0)$. The property can be invoked via an optimum choice of σ afterwards. The more complicated procedure that is followed below is designed to give better scaling properties. The ''best'' τ vs e curve will usually have a minimum, which we call $\tau_{\rm min}$.

(2) Define $q=z^\sigma(e-e_0)$; $f(q)$ has a maximum for some value of $q=\tilde{q}$: $f_{\rm max}=f(\tilde{q})$. For each z the yield $Y(z)$ as a function of e has a maximum at some value of $e_{\rm max}(z)$. At this excitation energy $Y(z)_{\rm max}=z^{-\tau}f_{\rm max}$, where $f_{\rm max}$ is a constant independent of z. This allows us to choose values for τ and $f_{\rm max}$ using a χ^2 test.

(3) The value of τ found above will be higher than $\tau_{\rm min}$. This means if we look for e appropriate for τ, two values are available from the τ vs e curve (see Fig. 1). The lower value is chosen as the value of e_0. The scaling property is badly violated by the other choice. The value of e_0 chosen by this prescription will be labeled e_1.

(4) Now that we know $e_0=e_1$ and $e_{\rm max}(z)$, the excitation at which each z is maximized, we find from a least squares fit the value of σ from the condition $z^\sigma(e_{\rm max}-e_1)=$const for all z.

(5) The scaling law can now be tested by plotting $Y(z)z^\tau$ vs $z^\sigma(e-e_1)$. Plots for all z should fall on the same graph.

Figure 1 depicts graphs [steps (1) to (3)] with and without the inclusion of the Coulomb force. In the graphs we also plot the specific heat per nucleon. We refer to the location of the maximum of specific heat as e_2. The lessons from LGM that we like to emphasize can be learned from Figs. 1 and 2. In Fig. 1 consider first the left panel (no-Coulomb case).

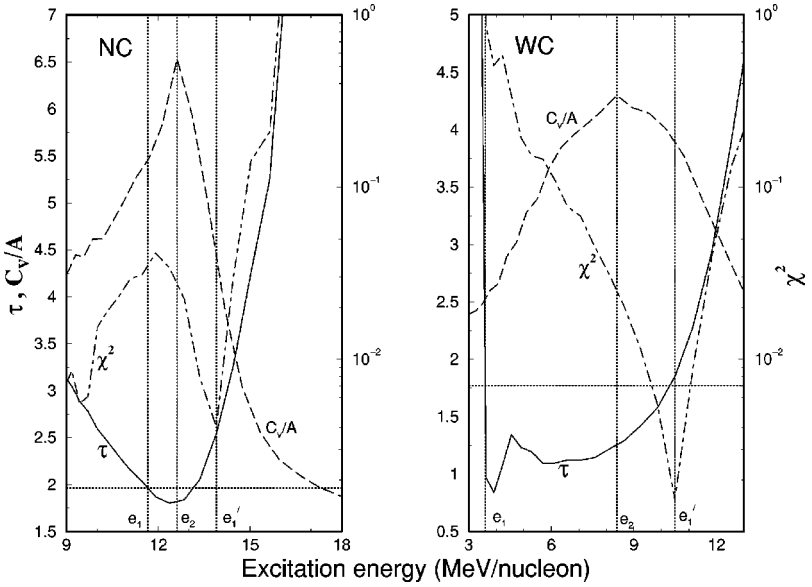

FIG. 1. In this figure we show "best" τ and χ^2 vs e [step (1), Sec. II] and also C_V vs e for the LGM calculation. The horizontal line below 2 is a straight line drawn at the value of τ from step (2), Sec. II. The locations e_1, e_2, and e_1' are the values of e for the scaling fit, maximum of specific heat, and the minimum of χ^2. The left panel is a LGM calculation without any Coulomb force; the right panel is with the inclusion of the Coulomb force. Notice the increase of $\Delta e = e_2 - e_1$ when Coulomb is included.

Here e_1 is 11.66 MeV, e_2 is 12.61 MeV, and e_1' [defined by the minimum of Ref. χ^2; the prescription of Ref. [14]; see part (1) above] is 13.88 MeV. The differences in values are small compared to the values themselves. With the Coulomb force e_1 drops well below e_2 and e_1'; e_2 and e_1' stay close.

In Fig. 3 we show that the scaling law is rather well obeyed around e_1. It is very poorly obeyed around e_1'. An interesting plot is the scaling law around e_2. This is also shown in Fig. 3. Of course the scaling around e_2 is nowhere as good as around e_1 but it is still better than around e_1' (not plotted).

Of the three energies e_1, e_2, and e_1', which one marks phase transition better? Without the Coulomb force, the $Y(z)$ curves have the same general shape, not displaying coexistence and overlap in the charge region used in the analysis. But with the Coulomb force, e_1 is clearly in the phase coexistence region and is below the phase transition energy (see Fig. 2). Looking at yields at e_2 and e_1', there is no obvious choice in deciding which marks the phase transition point better. However, since an extremum in the value of specific heat is a standard signature of phase transition, our preference is with e_2.

III. CALCULATIONS WITH A THERMODYNAMIC MODEL

Details of the thermodynamic model can be found in several places [1,6,7]. The physics assumption is that composites are formed at an appropriate temperature at a volume larger than normal nuclear volume dictated solely by consideration of phase space. Thus the model is close in spirit to the statistical multifragmentation model of Copenhagen [8] with the simplification that the freeze-out volume is assumed to be independent of the partitions. This allows for very quick computation without any Monte Carlo simulations. The inputs for this calculation are the following. Apart from

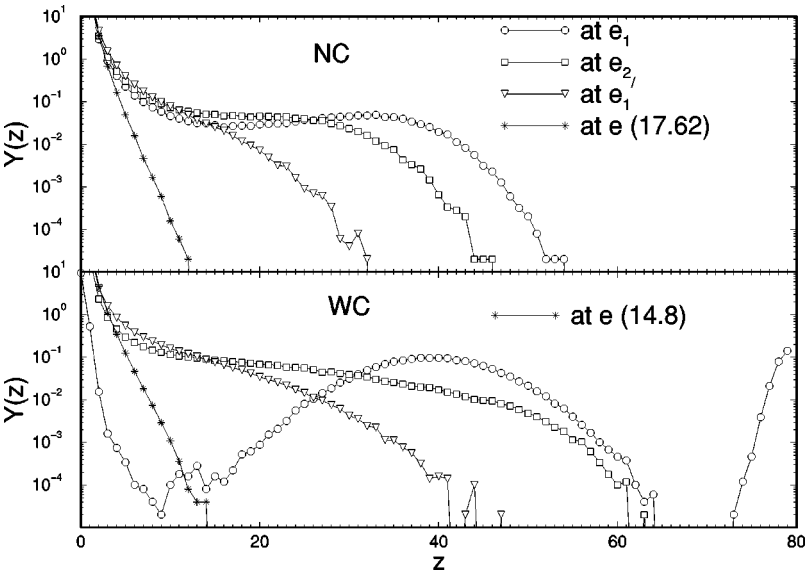

FIG. 2. LGM simulations for $Y(z)$ vs z at e_1, e_2, and e_1' without the Coulomb force (top panel) and with the Coulomb force (bottom panel). In the top panel both e_1 and e_2 are near the energy, where a maximum in the yield at the high z side has just disappeared. Qualitatively, this marks the phase transition point. But in the bottom panel where the Coulomb force is included, e_1 marks an energy when there is still a large fragment. Thus this is below the phase transition temperature. However, e_2 still marks the location when the maximum at the high z side has just disappeared. At much larger e values (shown arbitrarily at $e = 17.6$ MeV and $e = 14.8$ MeV), $Y(z)$ falls much more rapidly with z.

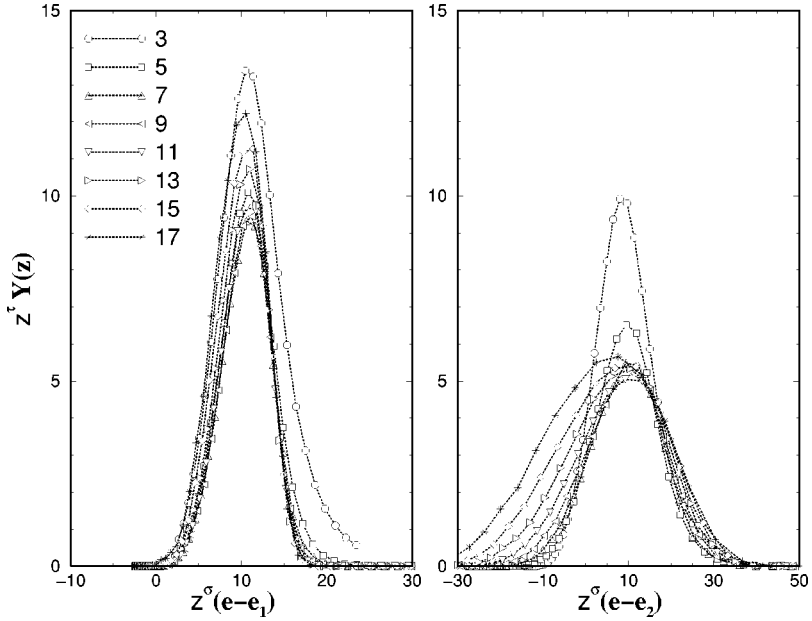

FIG. 3. For different isotopes z we plot $z^\tau Y(z)$ against $z^\sigma(e-e_1)$ in the LGM, where the exponent τ is the "best" τ at e_1 and extraction of σ, e_1 is described in the text. By scaling one means that curves for different z's coalesce into one. This is approximately true for scaling around e_1 (left panel) but not around e_2 (right panel). Scaling around e_1' is worse (not shown).

neutrons and protons, experimental binding energies and ground state spins are used for deuteron, triton, ^{3}He, and ^{4}He. No excited states are included for these. For mass 5 and higher we use the semiempirical formula for binding energies with volume term, surface tension term, symmetry energy, and Coulomb energy. Excited states for composites are included in the Fermi-gas approximation. The Coulomb interaction between different composites is included in the Wigner-Seitz approximation [8].

Since this is a canonical calculation, calculations are done for fixed temperatures. For each temperature, the average excitation energy per particle can be calculated. For comparisons with LGM, figures are drawn with energy as the abscissa. Table I gives both the temperature and energy for relevant quantities.

There is no reason to expect results close to the ones calculated using LGM. For example, e_1' is lower than e_2 in the thermodynamic model but higher in the LGM. Nonetheless, Fig. 4 shows that $\Delta e = e_2 - e_1$ increases significantly with inclusion of the Coulomb force (from 1.24 MeV to 5.28 MeV). Again e_1 does not seem to mark the point of phase transition at all (Fig. 5) and e_2 is a much better candidate. This is so in spite of the fact scaling is well obeyed with respect to e_1 and not so well with respect to e_2 or e_1' (Fig. 6).

TABLE I. The values of the parameters e_1, e_2, and e_1', corresponding T_1, T_2, and T_1', and τ's at these e_1, e_2, e_1' at e_1 as obtained in LGM and thermodynamic models, for the freeze-out density of $0.27\rho_0$. Values are shown for calculations with (WC) and without (NC) Coulomb interactions.

Parameters	LGM (NC)	LGM (WC)	THDM (NC)	THDM (WC)
e_1	11.66	3.60	6.77	0.75
T_1	4.46	1.95	7.53	2.94
$\tau(e_1)$	1.964	1.771	2.77	2.36
e_2	12.61	8.38	8.01	6.03
T_2	4.62	3.38	7.715	6.445
$\tau(e_2)$	1.824	1.251	2.44	1.55
e_1'	13.88	10.5	7.54	4.94
T_1'	4.88	3.82	7.65	6.05
$\tau(e_1')$	2.544	1.851	2.53	1.42

IV. 8 GeV/c π^- ON Au DATA

It is of interest to check if the conclusions reached in the theoretical models are verified in experimental data [15,16]. Several nontrivial issues need to be clarified before this can be attempted. Because the power-law fit is not exact, the extraction of τ from data or theoretical calculation has some ambiguity. In previous sections we calculated τ by minimizing the quantity defined as χ^2 in Eq. (2.1) at each e. But one could also minimize

$$\tilde{\chi}^2 \equiv \sum [Y(z) - Cz^{-\tau}]^2. \tag{4.1}$$

If one is using experimental data, a more standard practice would be to minimize [17]

$$\hat{\chi}^2 \equiv \sum \frac{[Y(z) - Cz^{-\tau}]^2}{\sigma(z)^2}, \tag{4.2}$$

where often the σ's are statistical errors. The difference in the value of τ extracted by minimizing Eq. (2.1) or Eq. (4.1) can be significant or small. In theoretically calculated values of $Y(z)$ the difference is small. But if we take the experimental values of $Y(z)$, a more significant difference in values is found depending on whether we use Eq. (2.1) or Eq. (4.1). For the experimental data of 8 GeV/c π^- on gold, the results of using Eqs. (2.1), (4.1), and (4.2) are shown in Fig. 7. One can give crude arguments that minimizing Eq. (2.1) rather than Eq. (4.1) means that $Y(z)$'s of higher z's are preferentially fitted. In [18], Eq. (4.2) was chosen.

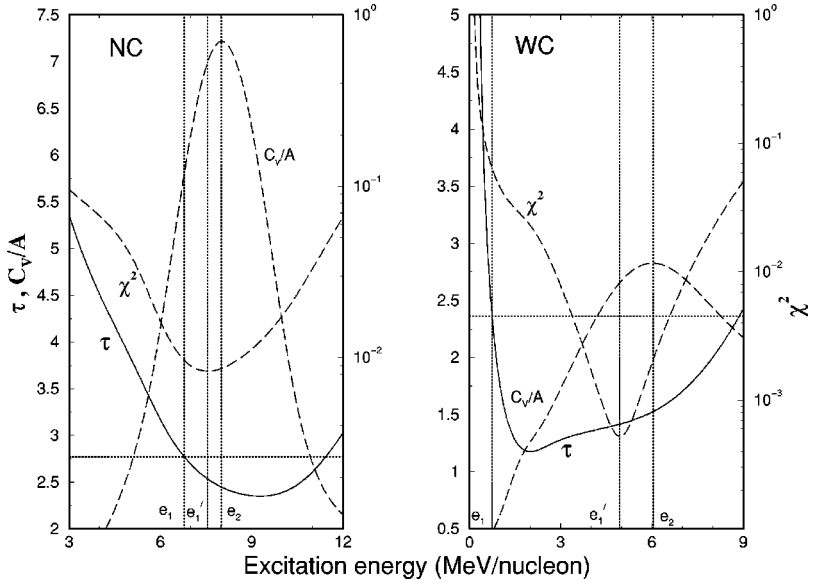

FIG. 4. Similar to Fig. 1 except the calculation is with the thermodynamic model (Sec. III), with a freeze-out density $0.27\rho_0$. Again note that with the inclusion of the Coulomb force (WC), $\Delta e = e_2 - e_1$ increases substantially compared to no Coulomb (NC) case.

In order to compare the experimental results to the theoretical calculations we have taken the experimental yields $Y(z)$'s, ignored all errors and repeated the calculations described in Sec. II. We show in Fig. 7 the results of this analysis. Qualitatively, the results are similar to the theoretical results (Figs. 1 and 4). In those two figures the minimum in τ occurs at very low excitation energy for the WC case. For the experimental data the minimum, if it exists, is also at a low value, below 1.5 MeV. More interesting is the right panel of Fig. 7 where we plot the experimental specific heat and find the maximum in specific heat coincides quite well with the minimum of χ^2 (this is e_1'). This agreement is also quite close to the theoretical predictions. The specific heat was extracted by differentiating with respect to T, the experimental caloric curve obtained for the same data set by Ruangma *et al.* [19].

We also test the scaling around e_1' (Fig. 8) although some qualifying comments need to be made about this figure. In experiments, the source size as well as the charge of the thermal source depend upon e. The scaling law, which spans e values on either side of e_1', assumes constant sources size as well as constant charge. Thus the scaling law cannot be directly tested without additional corrections renormalizing the yields $Y(z)$ to compensate for changes in the source size and charge. This was not done here. (However, the τ values and the values of χ^2 should be insensitive to such changes although we do require that for a given e, the source size and charge remain unchanged. This last condition is approximately obeyed.)

We can summarize the results of the comparison with experimental data as follows. In the data the maximum of specific heat (e_2) and the minimum of χ^2, e_1' both are e

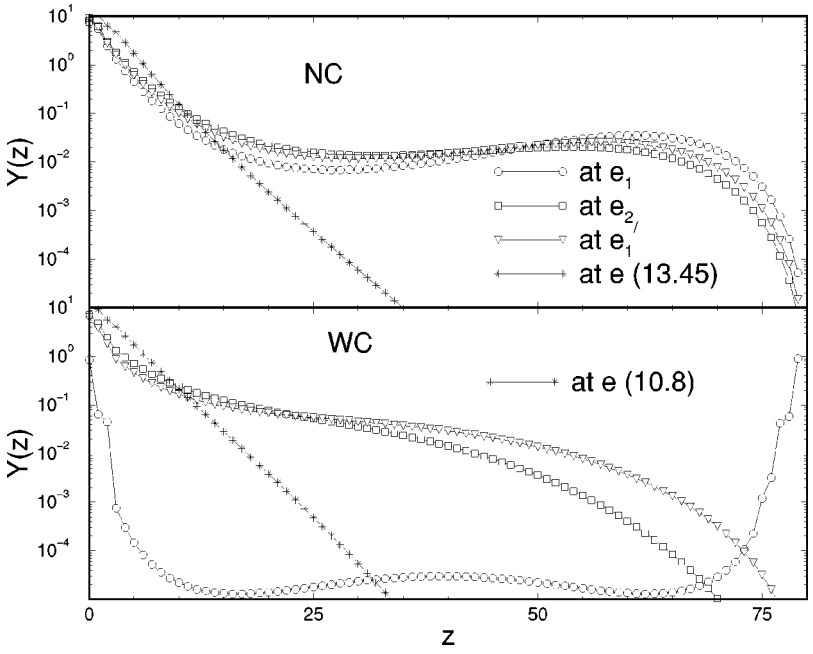

FIG. 5. Similar to Fig. 2 except the calculation is with the thermodynamic model (Sec. III). Again with (WC) and without (NC) the Coulomb interaction, e_2 continues to be a better mark for the point of phase transition energy. Without the Coulomb both e_1 and e_2 are acceptable. At higher energies (chosen arbitrarily at $e = 10.8$ MeV and 13.45 MeV) the drops of yields with z are much faster.

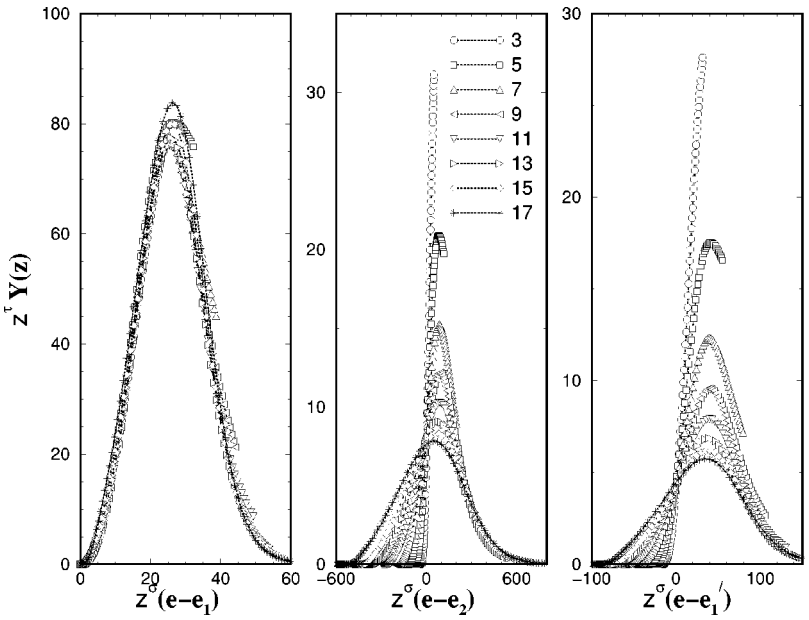

FIG. 6. Similar to Fig. 3 except that the thermodynamic model is used and scaling is tested around e_1, e_2, and e_1'.

$\approx 4MeV$ with a value of τ about 2.1 and σ about 0.53. This is very close to to the results of Elliott *et al.* [20] for the same data set using Fisher's droplet model approach and Berkenbusch *et al.* [21] using a percolation model. For percolation, the excitation energy was defined as the critical excitation energy in the sense of a second order phase transition. The thermodynamic model, which has no adjustable parameters and only a first order phase transition, reproduces trends of the data very well although both e_2 and σ are higher, 6 MeV and 0.96, respectively.

Since source sizes change with excitation per particle, we tested the sensitivity of model calculations with regard to size using the thermodynamic model. Table II gives the results. Within the range of variation of relevance to the experimental data the changes are small, though not negligible.

V. SUMMARY AND CONCLUSION

We have discussed three characteristic excitation energies (equivalently, temperatures): two of them have their origin in Eq. (1.2) (e_1 is the value of e_0 that gives the best scaling and e_1' is the value of e_0 where deviation from the power law is the least), and the third, e_2, is obtained from an extremum in the specific heat. In an ideal situation, all three would have the same value. In theoretical models they are close if the Coulomb force is omitted. The Coulomb force makes a substantial splitting between e_1 and e_1', indicating the sensitivity of the extracted thermodynamic quantities to this interaction. We find that e_1' gives a better measure of the phase transition energy and it stays close to e_2. In the experimental data that we considered e_1' and e_2 follow this pattern.

The quantitative results are dependent upon freeze-out densities and the source sizes but not sensitively so.

Lastly, we have not discussed the order of phase transition but the model calculations in Secs. II and III imply a first-order phase transition. In this interpretation, depending upon the excitation energy, most fragments are emitted while inside the coexistence region of the phase diagram (and possibly the spinodal region) and the extracted ''critical'' excita-

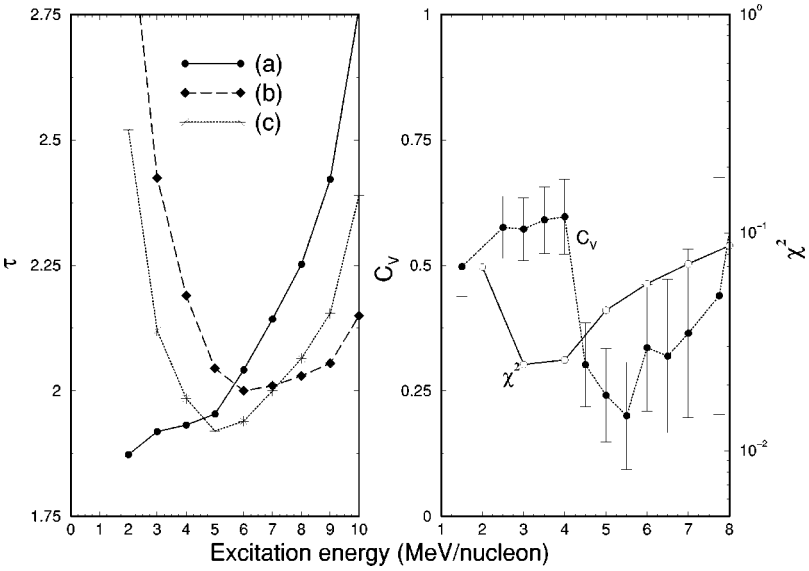

FIG. 7. The left panel shows the values of τ extracted from the ISiS data using three different fomulas: (a) by minimizing the right hand side of Eq. (2.1) at each e value, (b) by minimizing the right hand side of Eq. (4.1), and (c) by minimizing the right hand side of Eq. (4.2). In the right panel C_V from data and χ^2 [Eq. (2.1)] calculated from data are plotted. The minimum of χ^2 and maximum of C_V coincide within experimental uncertainty.

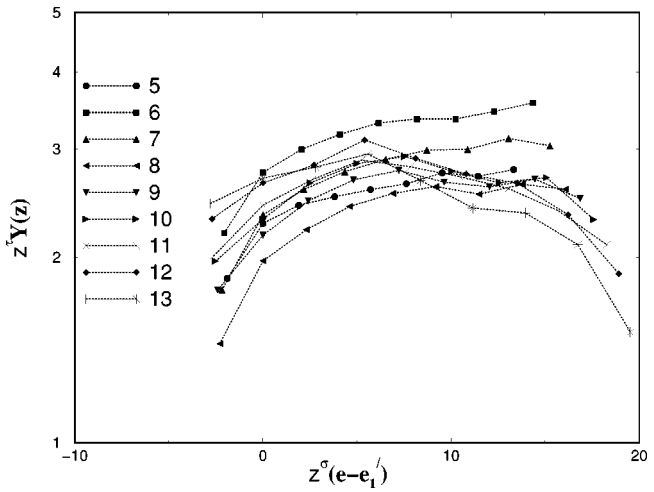

FIG. 8. Scaling behavior associated with the ISiS data, around e_1'.

tion energy indicates the boiling point. As pointed out earlier, the boiling point is at a similar excitation energy as the critical point found by Elliott *et al.* [20] from an analysis based on the Fisher droplet model and Berkenbusch *et al.* [21] based on percolation theory. Further discussions of critical phenomena [20,21] in disassembly of hot nuclei as opposed to first-order phase transition in the disassembly can be found in Refs. [12,22,23].

A first-order phase transition is consistent with recent observations by the ISiS collaboration [16,24,25] of a strong increase in fragment production probability, a strong decrease in fragment emission time, and the onset of collective radial expansion above 4*A* MeV of excitation energy, which were interpreted as signatures for bulk emission. It is also consistent with the flattening of the caloric curve from which the heat capacity was extracted [19].

TABLE II. The values of the parameters for two different sizes of the fragmenting source as obtained in the thermodynamic model, for a freeze-out density of $0.27\rho_0$.

Parameters	$N=118$ $Z=79$	$N=101$ $Z=68$
e_1	0.75	1.01
T_1	2.94	3.46
$\tau(e_1)$	2.36	2.35
e_2	6.03	5.90
T_2	6.445	6.40
$\tau(e_2)$	1.55	1.49
e_1'	4.94	4.91
T_1'	6.05	6.05
$\tau(e_1')$	1.42	1.41

ACKNOWLEDGMENTS

This work was supported in part by the Natural Sciences and Engineering Research Council of Canada and by *le Fonds pour la Formation de Chercheurs et l'aide à la Recherche du Québec*. Experiment E900 was supported by the U.S. Department of Energy and the National Science Foundation.

[1] S. Das Gupta, A. Z. Mekjian, and M. B. Tsang, Adv. Nucl. Phys. **26**, 91 (2001).
[2] D. Stauffer and A. Aharony, *Introduction to Percolation Theory* (Taylor and Francis, London, 1992).
[3] J. Pochodzalla *et al.*, Phys. Rev. Lett. **75**, 1040 (1995).
[4] A. Coniglio and W. Klein, J. Phys. A **13**, 2775 (1980).
[5] J. Pan and S. Das Gupta, Phys. Rev. C **51**, 1384 (1995).
[6] S. Das Gupta and A. Z. Mekjian, Phys. Rev. C **57**, 1361 (1998).
[7] P. Bhattacharyya, S. Das Gupta, and A. Z. Mekjian, Phys. Rev. C **60**, 054616 (1999).
[8] J. P. Bondorf, A. S. Botvina, A. S. Iljinov, I. N. Mishustin, and K. Sneppen, Phys. Rep. **257**, 133 (1995).
[9] C. B. Das, S. Das Gupta and S. K. Samaddar, Phys. Rev. C **63**, 011602(R) (2001).
[10] S. K. Samaddar and S. Das Gupta, Phys. Rev. C **61**, 034610 (2000).
[11] X. Campi and H. Krivine, Nucl. Phys. **A620**, 46 (1997).
[12] C. B. Das, S. Das Gupta and A. Majumder, Phys. Rev. C **65**, 034608 (2002).
[13] F. Gulminelli and Ph. Chomaz, Phys. Rev. Lett. **82**, 1402 (1999).
[14] R. P. Scharenberg *et al.*, Phys. Rev. C **64**, 054602 (2001).
[15] T. Lefort *et al.*, Phys. Rev. C **64**, 064603 (2001).
[16] L. Beaulieu *et al.*, Phys. Rev. C **64**, 064604 (2001).
[17] W. H. Press, B. P. Flannery, S. A. Teukolsky, and W. T. Vetterling, *Numerical Recipes* (Cambridge University Press, New York, 1987), p. 504.
[18] L. Beaulieu *et al.*, Phys. Lett. B **463**, 159 (1999).
[19] A. Ruangma *et al.*, nucl-ex/010004.
[20] J. B. Elliott *et al.*, Phys. Rev. Lett. **88**, 042701 (2002).
[21] M. K. Berkenbusch *et al.*, Phys. Rev. Lett. **88**, 022701 (2002).
[22] J. Pan, S. Das Gupta, and M. Grant, Phys. Rev. Lett. **80**, 1182 (1998).
[23] F. Gulminelli, Ph. Chomaz, M. Bruno, and M. D'Agostino, Phys. Rev. C **65**, 051601(R) (2002).
[24] L. Beaulieu *et al.*, Phys. Rev. Lett. **84**, 5971 (2000).
[25] T. Lefort *et al.*, Phys. Rev. C **62**, 031604(R) (2000).